

Boundary layer separation control on a highly-loaded, low-solidity compressor cascade

Zhou Yang, Liu Huo-xing, Zou Zheng-ping and Ye Jian

National Key Lab. on Aero-Engines, Aero-Engines Simulation Research Center, Beijing Univ. of Aero. & Astro., Beijing 100083

© Science Press and Institute of Engineering Thermophysics, CAS and Springer-Verlag Berlin Heidelberg 2010

Separated flow can be effectively controlled through the management of blade boundary layer development. Numerical simulations on a highly-loaded, low-solidity compressor cascade indicate that combined blowing and suction flow control technique can significantly improve cascade performance, especially in increasing the cascade loading and static pressure ratio as well as decreasing the loss coefficient. Meanwhile, it is more effective to improve cascade performance by blowing near leading edge on suction surface than suction near trailing edge. Both the locations and flow rates of blowing and suction are major impact factors of this method to cascade performance. Comparing to the baseline, the static pressure ratio increases by 15% and loss coefficient decreases by 80%, with a blowing fraction of 1.7% and a suction fraction of 1.38% of the inlet mass flow.

Keywords: combined blowing and suction, flow control, compressor cascade, boundary layer, separated flow

Introduction

In recent compressor designing, the trend is to attain high stage or single-blade-row loading. The main paths to enhance single-stage or single-blade-row aerodynamic loading are to increase compressor blade tip velocity or diffusion factors [1]. However, the increasing of blade tip velocity is limited by the centrifugal stress in blades, the blades durability, the compressor surge margin, the noise, etc. It is clear that the potential improvement of compressor blade tip velocity is nearly being approached. Thus, the effective way to enhance compressor loading is to increase the compressor diffusion factors. But there are still some problems in increasing diffusion factors [2]. High diffusion factors means large adverse pressure gradient, then flow in boundary layer on suction surface may separate which decreases static pressure ratio, through-flow mass flow rate, efficiency and operating range. How

to suppress compressor blade boundary layer separation becomes one of the most important techniques to enhance engine performance.

It is effective to suppress flow separation by flow control technique. Flow control techniques used in external flow such as in airfoil have attained great success. Typical techniques include rotating cylinder at leading and trailing edge, circulation control by tangential blowing at leading and trailing edge, multi-element airfoils, jet flow at leading edge, etc. By blowing near leading edge and suction near trailing edge on the suction surface of the airfoil, Zha's research successfully demonstrated the superior performance of co-flow jet airfoil concept. Compared with the baseline airfoil, the maximum lift increased by 113%, the angle of attack operating range increased by 100%, and the minimum drag coefficient reduced 30% at least [3,4].

Based on the success of flow control in the external

flows, several researches of flow control in fan/compressor blade have been established. In fan/compressor design, the aerodynamic loading can be significantly improved by aspirating low-velocity fluid out boundary layer or injecting high energy fluid into boundary layer. This flow control technique becomes one of the hottest topics all over the world. Dennis investigated the effects of active flow separation control on a stator vane and found separation reduced and total pressure loss of 25% were reduced by injection on the suction surface [5]. The research work of MIT Gas Turbine Laboratory on aspirated compressors gained great success [6-10]. They had first designed two single-stage aspirated compressors, one was a transonic aspirated compressor stage, designed to achieve a pressure ratio of 1.6 at a blade speed of 750 ft/sec, the other was a high pressure ratio aspirated compressor stage, designed to achieve a pressure ratio of 3.5 at a blade speed of 1500 ft/sec. The rotor efficiency of the aspirated compressor reached 96% and stator reached 90% when the aspirated mass flow rate was 4.7% of the passage throughflow, approximately 1.0% aspirated through slots on suction surface of the rotor and stator blades, the remainder distributed over the rotor shroud and stator hub [6]. The experimental investigation of this compressor illustrated that through-flow efficiency at the design point achieved 90% and good performance at off-design point achieved [7]. The high pressure aspirated compressor achieved an isentropic efficiency of 86% when the aspirated mass flow rate was 7% of the passage throughflow, approximated 4% on suction surface and 3% on the hub and shroud near shock impingement [8]. The 3D viscous computational prediction at off-design conditions also showed good performance [9]. Then they designed a two-stage counter-rotating fan with a pressure ratio of 3 and adiabatic efficiency of 89% by employing suction on the second rotor blades extended from the hub to 80% span, and the test attained an overall polytropic efficiency better than 90% [10]. Carter designed and tested a compressor stator with boundary layer suction and blowing, and a reduction of 65% of loss coefficient was achieved when blowing mass flow rate was 1.6% of the passage throughflow [11]. Dang designed aspirated compressor blades using 3D inverse method, and found a minimum of sucked flow that required for a performance improvement at design and off-design operations [12]. Chen first concentrated their researches on the position of suction slot. They found out the best location to enhance the performance. And they also discussed the effect of solidity on performance. The results indicated that the overall performance of cascade influenced by solidity combined with incidence, suction slot location and suction mass flow rate [13-15].

Flow control techniques used in fan/compressor have also attained great success. However, the generally em-

ployed methods in fan/compressor flow control were blowing only or suction only method, the method of combined blowing and suction flow control technique rarely applied to boundary layer control in fan/compressor [11].

The work presented below is the numerical analysis of a two-dimensional highly-loaded compressor cascade employing combined blowing and suction flow control technique. The effects of blowing slot location, suction slot location and blowing flow rate to the overall performance are analyzed in detail respectively.

The structure of this paper is as follows: The physical model and computational method are summarized first, followed by grid-dependence study. Then the detail analysis of the flow structure is described. Lastly, the important conclusions are enumerated.

Geometry construction

A compressor cascade profile was designed to investigate the effects of combined blowing and suction technique on cascade performance. Figure 1 shows the configuration of the profile and zoomed-in meshes near blade leading and trailing edge. NACA0012 airfoil was selected as baseline and arc as camber line. Considering the internal ducts of blowing and suction slots, the cascade trailing edge was thickened. The chord was chosen as 113.2mm. To improve the cascade aerodynamic loading, 60 degree was selected for blade camber angle and 0.87 for solidity. As the cascade got very large camber angle under low solidity, the aerodynamic loading was much higher than conventional ones. In this paper combined blowing and suction technique was used to control the flow separation of boundary layer, meanwhile, the suction surface of the cascade is also changed to some degree, the new suction surface shape is a downward translation of the portion of the original suction surface between the blowing and suction slot. As shown in Figure 1, the baseline and final cascade geometry is drawn in dashed and solid line respectively. The blowing slot is located at 3%, 8%, 17% of the chord from leading

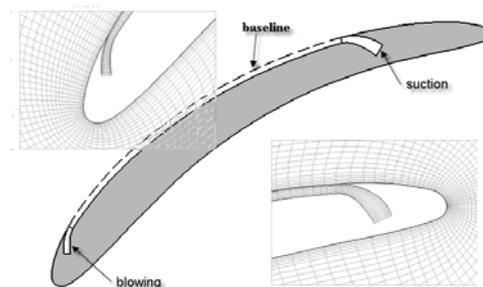


Figure 1 Schematic blade configuration and mesh around leading edge and trailing edge

edge and suction slot is located at 52%, 73%, 90% chord positions. The width of blowing and suction slot is 0.96% and 1.12% of the chord respectively. The slot faces are normal to the suction surface to make the flow tangential to main flow.

NUMECA Fine/Turbo was used to calculate the cascade flowfield. Steady RANS equations were solved by time-marching finite volume method, spatial discretizations were central difference and time advancement was fourth-order Runge-Kutta method, full multigrid techniques were used for convergence accelerating. Spalart-Almarras turbulence model was used. The total temperature, total pressure and inlet angle at inlet was set the same for all cases, backpressure was altered slightly to ensure the cascade inlet Mach number was constant for all cases. The computational domain length is 6 times of the chord, and the length from the inlet to the cascade leading edge is 1.5 times. Two dimensional computational meshes are generated by IGG with total number about 26000. With an ‘‘H-O-H’’ type structure, it is relatively easy to control the grid density and to improve mesh orthogonality. The peak wall y^+ is below 10. The Reynolds number based on the chord and the inlet flow velocity is 1.5×10^6 .

Grid-dependence study

The simulation of baseline (shown in Figure 1 in dashed line) on three kinds of grids has been taken, the flow conditions are the same to case 1 in the following section. The cascade static pressure ratio (Ps), total pressure aerodynamic loss (Yp) and diffusion factor (DF) in these cases are listed in Table 1. The static pressure ratio is defined by static pressure at cascade inlet divided by static pressure at cascade outlet, and the total pressure aerodynamic loss is defined in equation 1.

$$Y_p = \frac{P_{in}^* - P_{out}^*}{\frac{1}{2} \rho \cdot U_{ref}^2} \quad (1)$$

Where U_{ref} (the reference velocity) is the velocity at cascade inlet. P_{in}^* and P_{out}^* is total pressure at cascade inlet and outlet. The diffusion factor is defined in equation 2.

$$DF = 1 - \frac{V_2}{V_1} + \frac{\Delta V_u}{2\tau \cdot V_1} \quad (2)$$

Where V_1 , V_2 are the velocity at cascade inlet and outlet respectively, ΔV_u is the tangential velocity change across the cascade, τ is the cascade solidity.

It can be seen from Table 1 that medium density grid are sufficient for numerical simulation of this 2D compressor cascade. Compared with simulation result with medium density grid, the static pressure ratio, aerodynamic loss coefficient and diffusion factor of coarse den-

sity grid is 1.7%, 6.2% and 10.4% higher respectively. However, the fine one of Ps and DF maintains unchanged, only Yp increases 1.6%. Thus, the results of the medium density grid can be viewed as grid independence. And numerical simulations in the following of the paper choose the medium density grid.

Table 1 Grid-dependence study

	Ps	Yp	DF	Grid number
Coarse	1.16	0.068	0.53	12870
Medium	1.14	0.064	0.48	22880
Fine	1.14	0.065	0.48	37990

Discussion of the results

The cascade performance can be affected by many factors of flow control technique, such as mass flow rate of blowing or suction, locations of blowing or suction, etc. In order to obtain details concerning effects of each factor, what follows will concentrate on the following major aspects: blowing slot location, suction mass flow rate, suction slot location and blowing mass flow rate.

Effect of blowing slot location

The simulation of baseline was first processed. Vector lines and M contour of baseline is presented in Figure 2. It is found that flow became supersonic at the location of 2% from leading edge on suction surface, and then flow accelerated quickly until 8% chord from leading edge where an intense shock appeared. At the location of 15% chord, flow started to separate. Thus, three typical blowing slot locations were selected as following:

Case A: blowing slot located at 3% of the chord from leading edge.

Case B: blowing slot located at 8% of the chord from leading edge.

Case C: blowing slot located at 17% of the chord from leading edge.

Overall cascade performance was presented in Table 2. It can be concluded that location of the blowing slot

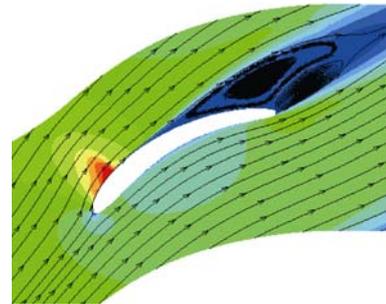


Figure 2 Vector lines and Mach contour of baseline

Table 2 Overall cascade performance (blowing slot location varied)

	M	P_s	Y_p	DF	Blowing fraction
baseline	0.73	1.16	0.0690	0.52	0
Case A	0.73	1.296	0.0174	0.803	1.74%
Case B	0.73	1.297	0.0147	0.806	1.75%
Case C	0.73	1.291	0.0160	0.792	1.73%

showed great effect to the overall cascade performance. The blowing slot located slightly behind the point where intense shock appeared showed great improvement of the overall performance, and static pressure ratio increased by 11.8%, total pressure loss decreased to 22%. Thus, blowing slot location was selected as case B described in the following of the paper.

Effect of suction mass flow rate and suction slot location

In this section, six simulations are presented:

Case 1: baseline, namely the case with neither blowing nor suction, the geometry is not translated, as shown in Fig.1 by the broken line.

Case 2: blowing only method employed, and the blowing slot located at 8% of the chord from leading edge.

Case 3: combined blowing and suction method employed, and the blowing and suction slot located at 8% and 52% of the chord from leading edge respectively.

Case 4: the same geometry as case 3 with different suction mass flow.

Case 5: combined blowing and suction method employed, and the blowing and suction slot located at 8% and 73% of the chord from leading edge respectively.

Case 6: combined blowing and suction method employed, and the blowing and suction slot located at 8% and 90% of the chord from leading edge respectively.

In the six cases, the total temperature and total pressure at mainflow inlet, blowing slot inlet and suction slot outlet are held constant. Backpressure of the mainflow is altered slightly to ensure the Mach number at cascade leading edge maintaining at 0.73 for the six cases.

Table 3 illustrates overall cascade performance of the

six cases. It can be seen from it that, compared to the baseline, the cascade aerodynamic loading improved dramatically by employing combined blowing and suction flow control. These improvements lay mainly in three aspects. First, the cascade static pressure ratio increased by 15%; secondly, the diffusion factor reached 0.82; lastly, the cascade aerodynamic loss coefficient decreased by 81%. The most important reasons are as follows. On the one hand, a high energy jet is injected tangentially near leading edge, which can increase cascade circulation; on the other hand, the turbulence shear layer between the high energy jet and mainflow causes strong turbulence diffusion and mixing, which enhances lateral transport of energy from the jet to mainflow and allows mainflow to overcome severe adverse pressure gradient and suppresses separation.

It can be concluded from above analysis that combined blowing and suction method is effective. However, the cascade performance varied as the location of suction slot and suction mass flow rates varied. The effects of each factor will be analyzed specifically as follows:

The suction mass flow rate will be discussed firstly for its subordinate effect. It can be seen from the comparison between case 3 and case 4 that cascade performance, such as static pressure ratio, aerodynamic loss coefficient and diffusion factor rarely changed when the suction mass flow rate changed from 1.38% to 1.53% solely. However, comparing case 4 and case 5, it can be seen that cascade performance improved obviously when the position of suction slot changed from 52% to 73% chord length while cascade inlet Mach number, blowing and suction mass flow rate were fixed. From these two group comparisons, the results indicate that the position of the suction slot dominates to the mass flow of suction in improving cascade overall flow properties while blowing slot location is fixed.

The change of the suction slot location influences flowfield dramatically when the cascade inlet Mach number, blowing slot location and blowing mass flow rate are held constant. Comparing case 4, case 5 and case 6, it can be seen that there is an optimal location of suction slot when employing combined blowing and suction flow control technique, and the optimal location is

Table 3 Overall Cascade Performance

	M	P_s	Y_p	DF	Blowing fraction	Suction fraction
Case1	0.73	1.16	0.069	0.52	0	0
Case2	0.73	1.24	0.043	0.67	1.74%	0
Case3	0.73	1.29	0.019	0.77	1.72%	1.53%
Case4	0.73	1.29	0.021	0.77	1.72%	1.38%
Case5	0.73	1.31	0.013	0.82	1.73%	1.38%
Case6	0.73	1.25	0.039	0.68	1.71%	1.00%

slight behind the separation position on suction surface (in this paper the optimal location is located at 73% of the chord). The existence of this critical location can be explained that the blowing and suction flow are tangential to the baseline of the suction surface. Meanwhile, the suction surface between blowing slot and suction slot is a downward translation of the portion of the original surface when use of boundary layer control, and then not only a large mass flow rate of low energy fluid in the boundary layer could be aspirated but also mainflow kept attached to the suction surface after the suction slot (see Figure 3 (a)). It could also be deduced that the suction slot location after the optimal location showed little effect on improving the cascade performance, the aerodynamic loading rarely increased. There are two reasons for this: first, as shown in Figure 3 (b), there is a recirculation region that caused the aspirated fluid opposite to the suction inlet, and it increased loss and decreased aspirated mass flow rate; secondly, it is very difficult to make separated flow reattached to the surface because of the diffusion of flow separation.

Figure 4 shows surface isentropic Mach number distribution of five cases (due to the fact that the cascade geometry of case 3 and case 4 are the same, case 4 was ignored.). It can be seen from it that the peak Mach number at leading edge of suction surface is approximately 1.4 in all cases, and this phenomenon is mainly

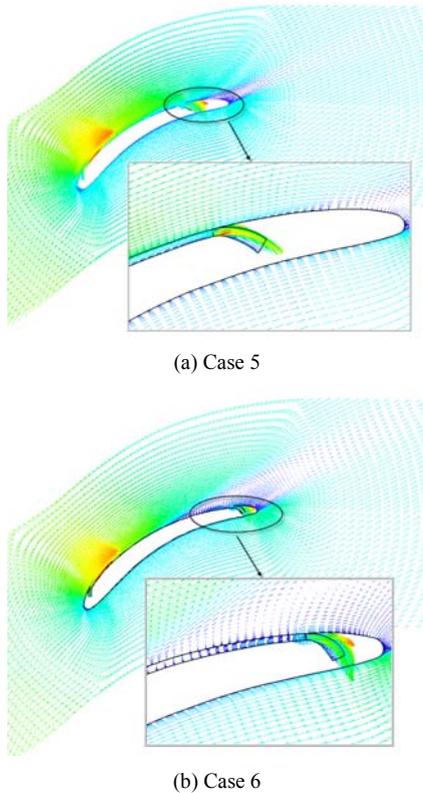


Figure 3 Vector line around trailing edge

caused by flow acceleration around leading edge surface and blowing at leading edge. From the distribution of isentropic Mach number shown in Figure 4, it could be deduced that there are two main changes by employing boundary layer control. First, aerodynamic loading improved over full chord range. Because the suction slot location changed, surface isentropic Mach number distribution changed. Case 5 showed the highest performance mainly because of the flow turning angle increased mostly; secondly, the more reasonable distribution of isentropic Mach number on suction surface attained. In case 1, the isentropic Mach number distribution on rear part of suction surface was almost unchanged, but in other cases, it decreased smoothly after the peak Mach number till the trailing edge. In case 1, the severe flow separation on rear part of suction surface made the cascade compressing capability lost, while in other cases, as seen in Figure 5, the severe flow separation was suppressed by employing boundary layer control. Figure 5 shows the streamline and contour of Mach number of each case, in case 1, flow separation started from the position of the peak Mach number, and a large low-velocity region existed. However, flow separation moved back to the trailing edge obviously by employing boundary layer control. Meanwhile, low-velocity region was reduced. When suction slot was near the optimal position, the flow reached the perfect state which could be seen from Figure 5 (d). But because the trailing edge was too thick, there was still a finite low-velocity region around the trailing edge.

Effect of blowing mass flow rate

The former section indicates that the optimal suction slot location is slightly behind flow separation position, and the location of suction slot is more important than the suction mass flow rate in flow separation control. This section will discuss the cascade performance due to the variety of blowing mass flow when blowing slot is located at the optimal position.

Figure 6 shows static pressure ratio and aerodynamic loss coefficient changed with blowing mass flow rate

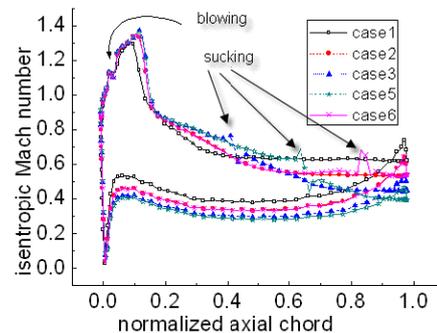


Figure 4 Surface isentropic Mach number distribution

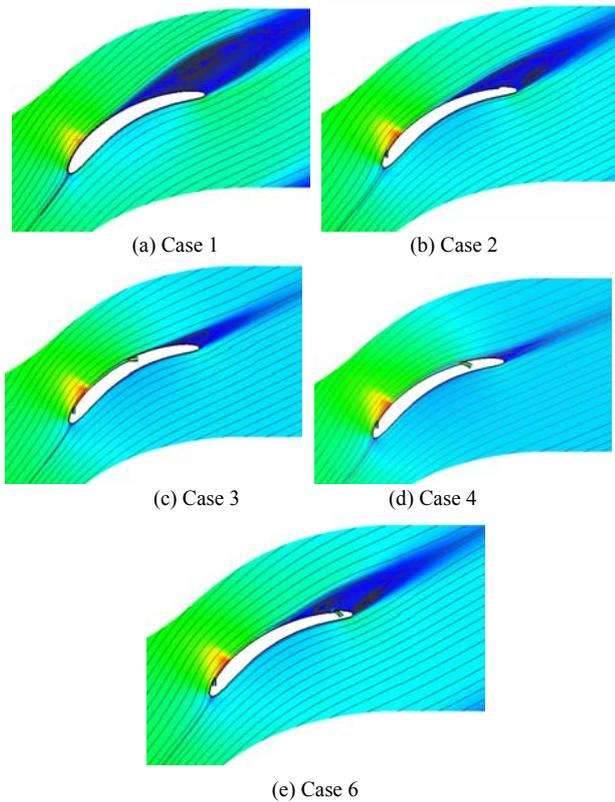


Figure 5 Streamline and Mach number contour

(normalized by cascade inlet mass flow) when suction slot located at 73% of the chord from leading edge. It is observed that there is a critical value of blowing mass flow rate to the improvement of cascade performance, which turns out to be 1.61% in this paper. Below the critical point, increasing the blowing mass flow rate will enhance cascade performance significantly. However, if the blowing mass flow rate exceeds the critical value, increasing the blowing mass flow rate rarely enhance cascade performance. When blowing mass flow rate varied from 1.53% to 1.61%, the static pressure ratio increased dramatically from 1.16 to 1.30 and aerodynamic loss coefficient decreased from 0.058 to 0.012. Contrary to this, when the blowing mass flow rate varied from 1.61% to 1.73%, the cascade flow properties rarely improved. From Figure 5, it can be seen that P_s increased no more than 0.4% and Y_p just decreased from 16.6% to 14.3% (normalized by Y_p of baseline). That is to say that the cascade has reached its aerodynamic loading limit.

Figure 7 shows the contours of Mach number when blowing mass flow rate is 1.61% and 1.55%, obviously, a large low-velocity region exists at lower blowing mass flow rate (as shown in Figure 7 (b)). And this low-velocity region combined with boundary layer on suction surface caused great loss, which can be seen from contours of entropy shown in Figure 8. However, when blowing

mass flow rate is higher than critical value of blowing mass flow rate, low-velocity region appears to stay around trailing edge. In this condition, while the cascade reaches its aerodynamic loading limit, blowing jet only affects low-velocity fluid, but P_s and Y_p rarely changed (which can be seen from Figure 6). From the above analysis, it can be obtained that flow separation position can be controlled by blowing or suction while the cascade inlet velocity and cascade geometry are fixed. When the cascade geometry is fixed, although the varied cascade inlet flow velocity changed the optimal suction slot position, the boundary layer flow separation could still be controlled by adjusting blowing mass flow rate.

Effect to cascade operating range

The combined blowing and suction flow control technique not only improves cascade performance when the inlet Mach number is fixed (such as increasing P_s and decreasing Y_p), but also extends cascade operating range

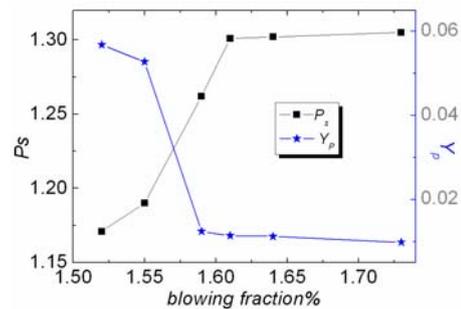


Figure 6 Static pressure ratio and loss coefficient due to different blowing fraction

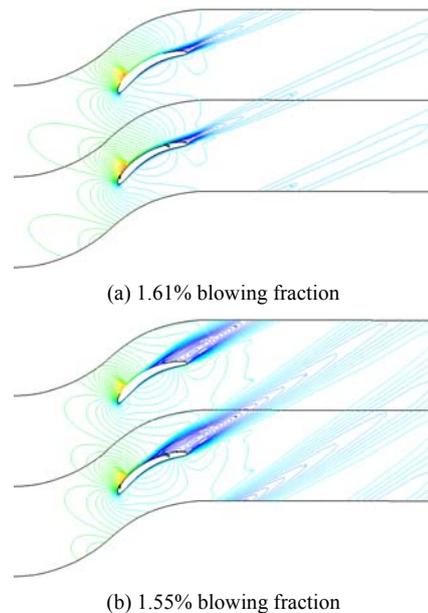


Figure 7 Contours of Mach number

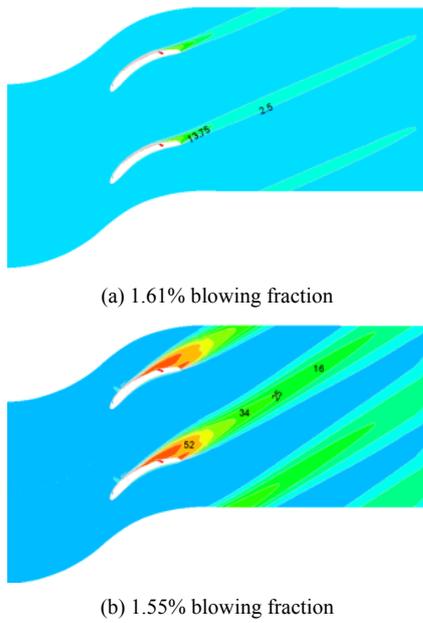


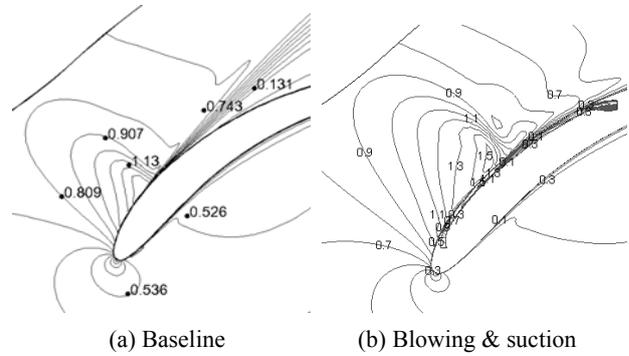
Figure 8 Contours of entropy

and improves cascade performance at inlet Mach number limitation (the highest inlet Mach number that could be reached).

Table 4 shows the comparison of P_s , Y_p and DF under inlet Mach number limitation between baseline and the case that employing combined blowing and suction (blowing and suction slots located at 8% and 52% of the chord from leading edge respectively). The table illustrates that inlet Mach number limitation of the latter (combined blowing and suction) is higher than the former case (baseline), which means that cascade aerodynamic loading limit is improved, Y_p decreased 40%, P_s increased 20% and DF increased from below 0.4 to 0.76. This is mainly caused by reduction of flow separation region. Figure 9 (a) illustrates that the low-velocity region starts from the maximum thickness of the cascade in baseline, and then expands to almost the whole flow passage. The supersonic flow appears near the leading edge of suction side and induces a shock, and the shock interacting with boundary layer induces flow separation that can not reattach to suction surface. While in the latter case, though the interaction between shock and boundary layer still exists, transport of energy from the high-energy injected flow suppresses the flow separation and eliminates low-velocity region, and then the inlet Mach number limitation could be increased due to the fact that the cascade could pass a significantly large mass flow rate. However, there are two factors restrict inlet Mach number limitation to become even higher. First, flow properties rarely improved when blowing mass flow rate is higher than critical value; secondly, there is a large region in cascade suction side that flow becomes supersonic

Table 4 Performance comparison at inlet Mach number limit

	M	P_s	Y_p	DF
Baseline	0.76	1.09	0.091	0.38
Blowing & Suction	0.83	1.36	0.049	0.76



aerodynamic loss maintained, the static pressure ratio increased by 20%.

Acknowledgments

The present research was carried out under the support from the National Natural Science Foundation of China as part of the Free Application Project (No. 50776003). Some of the work of this research has been supported and funded by the Key Program of Aviation Science Foundation, Grant No.2007ZB51018

References

- [1] Chen M.Z., Development of fan/compressor techniques and suggestions on further researches, *Journal of Aerospace Power*, 2002, 17(1): 1–15.
- [2] Cumpsty N.A., *Compressor aerodynamics*, Longman Scientific & Technical, New York, 1st Edition, 1989.
- [3] Zha G.C. and Paxton.C, A novel airfoil circulation augment flow control method using co-flow jet, *AIAA Paper* 2004–2208.
- [4] Zha G.C., Carroll B.F., Paxton C.D., et al, High performance airfoil using co-flow jet flow control, *AIAA Paper* 2005–1260.
- [5] Dennis E.C., Michelle M.B., Patricia S.P., et al, Active flow separation control of a stator vane using embedded injection in a multistage compressor experiment, *Journal of Turbomachinery*, 2004, 126: 24–34.
- [6] Schuler B.J., Kerrebrock J.L., Merchant A.A., et al, Design, analysis, fabrication and test of an aspirated fan stage, *ASME paper* 2000-GT-618.
- [7] Schuler B.J., Kerrebrock J.L., Merchant A.A., Experimental investigation of a transonic aspirated compressor, *Journal of Turbomachinery*, 2005, 127: 340–348.
- [8] Merchant A.A., Drela M., Kerrebrock J.L., et al, Design and analysis of a high pressure ratio aspirated compressor stage, *ASME Paper* 2000-GT-619.
- [9] Merchant A. A.; Kerrebrock J. L.; Adamczyk J. J., et al, Experimental investigation of a high pressure ratio aspirated fan stage, *ASME Paper* 2004-GT-53679.
- [10] Kerrebrock J.L., Epstein A.H., Merchant A.A., et al, Design and test of an aspirated counter-rotating fan, *ASME Paper* GT-2006-90582.
- [11] Carter C.J., Guillot S.A., Ng W.F., Aerodynamic performance of a high-turning compressor stator with flow control, *AIAA Paper* 2001–3973.
- [12] Dang T.Q., Van Rooij M.P.C., Larosiliere L.M., Design of aspirated compressor blades using three-dimensional inverse method, *ASME Paper* GT-2003-38492.
- [13] Chen F., Song Y.P., Zhao G.J., et al, Effects of boundary layer suction on the performance of compressors cascade with different solidities, *Journal of Engineering Thermophysics*, 2005, 26(2): 211–215.
- [14] Song Y.P., Chen F., Zhao G.J., et al, Numerical investigation of boundary layer suction in compressor cascade with large turning angles, *Journal of Aerospace Power*, 2005, 20(4); 561–566
- [15] Song Y.F., Chen F., Liu J. et al, Off-design performance of compressor cascade with boundary layer suction, *Journal of Engineering Thermophysics*, 2006, 27(4); 589–591.